Endocytosed β-VLDL and LDL Are Delivered to Different Intracellular Vesicles in Mouse Peritoneal Macrophages

Ira Tabas,*‡ Sungtae Lim,§ Xiang-Xi Xu,* and Frederick R. Maxfield‖§

Departments of *Medicine, ‖Pathology, ‡Cell Biology, and §Physiology and the §Institute of Human Nutrition, Columbia University, New York 10032

Abstract. Hypercholesterolemic rabbit β-VLDL and human LDL are both internalized by mouse peritoneal macrophages by receptor-mediated endocytosis. However, only β-VLDL (which binds to the cells with a much higher affinity than LDL) markedly stimulates acyl-CoA/cholesterol acyl transferase (ACAT) and induces foam cell formation in these cells. As an initial step to test whether the two lipoproteins might be targeted to different organelles (which might differ in their ability to deliver cholesterol to microsomal ACAT), we studied the endocytic pathways of β-VLDL and LDL. Lipoproteins were labeled with the non-transferable fluorescent label, DiI. When the macrophages were incubated with DiI-LDL for 10 min at 37°C, the fluorescence was concentrated near the center of the cell both in heavily labeled vesicles and in a diffuse pattern. The pattern with DiI-β-VLDL was quite different: an array of bright vesicles throughout the cytoplasm was the predominant feature. Differences in distribution were seen as early as 2 min of incubation and persisted throughout a 10-min chase period. By using a procedure in which photobleaching of DiI fluorescence converts diaminobenzidine into an electron-dense marker, we were able to identify at the ultrastructural level vesicles containing electron-dense material in cells incubated with DiI-β-VLDL. Human E2/E2 β-VLDL (from a patient with familial dysbetalipoproteinemia), which has a binding affinity and ACAT-stimulatory potential similar to LDL, gave a pattern of fluorescence virtually identical to LDL. Pulse-chase studies with ^{125}I-labeled and [^{3}H]cholesteryl ester-labeled lipoproteins disclosed that both protein degradation and cholesteryl ester hydrolysis were markedly retarded in β-VLDL compared with LDL. Thus, in mouse peritoneal macrophages, endocytosed β-VLDL appears in a distinct set of widely-distributed vesicles not seen with LDL (or with E2-β-VLDL) and, compared with LDL, has a markedly diminished rate of protein degradation and cholesteryl ester hydrolysis. The differential routing of LDL and β-VLDL may provide a mechanism for differences in ACAT-stimulatory potential between the two lipoproteins.

CHOLESTERYL ester (CE)[1]-loaded macrophages, or foam cells, are a prominent feature of atherosclerotic lesions (10, 11, 30). The precise cellular and molecular mechanisms of macrophage CE accumulation are as yet unknown. In a widely studied tissue culture macrophage, the mouse peritoneal macrophage, CE accumulation can occur with modified forms of LDL (e.g., acetylated LDL) (4) and with CE-rich $d < 1.006$ g/ml lipoproteins from hypercholesterolemic animals (β-VLDL) (24). However, CE accumulation does not occur with native LDL (5) despite significant LDL uptake and degradation by the cells (33). In each case where CE accumulation occurs, the intracellular cholesterol esterification pathway, catalyzed by the enzyme acyl-CoA/cholesterol acyl transferase (ACAT), is stimulated (4). For these and other reasons (34), the ACAT pathway is thought to play a critical role in macrophage foam cell formation. Although the properties and regulation of ACAT, which has not yet been purified, are poorly understood, the process of intracellular delivery of lipoprotein-derived cholesterol (reviewed in reference 32) and cellular cholesterol (5, 36) to the microsomal ACAT enzyme is thought to be a key step involved in its stimulation.

The lipoproteins which interact with macrophages bind to specific cell surface receptors and enter the cell by the process of receptor-mediated endocytosis (4). Interestingly, there is considerable evidence to suggest that LDL, which poorly stimulates ACAT, and β-VLDL, which is a potent stimulator of ACAT, enter mouse peritoneal macrophages by the same receptor (9, 21). This receptor is a protein that is very similar to the human fibroblast LDL, or apo-B,E, receptor (9, 21). Whether or not this protein is, in fact, responsible for internalizing both LDL and β-VLDL, an important difference does exist in the interaction of the two li-

1. *Abbreviations used in this paper*: ACAT, acyl-CoA/cholesterol acyl transferase; CE, cholesteryl ester; DiI, 1,1'-dioctadecyl-3,3,3',3'-tetramethylindocarbocyanine percholate; DiO, 3,3'-dioctadecyloxacarba-cyanine perchlorate; LPDS, lipoprotein-deficient serum.

poproteins with macrophages: β-VLDL, via its ligand, apo E, binds to the cell surface with a much higher affinity than LDL, whose ligand is apo B.

Although there has been considerable progress made both in understanding the interaction of LDL and β-VLDL with the macrophage cell surface (9, 21) and in elucidating the endocytic pathway of LDL in non-macrophage cells (reviewed in reference 16), little is known about the endocytic pathways of LDL and β-VLDL in macrophages. We reasoned that information about these pathways might eventually help explain the marked differences between LDL and β-VLDL in their ability to stimulate ACAT. For instance, LDL and β-VLDL might be targeted to different subpopulations of organelles that, in turn, might differ in their ability to transfer lipoprotein-derived cholesterol to microsomal ACAT. We now present morphological and biochemical data which examines the early endocytic pathways of LDL and β-VLDL in mouse peritoneal macrophages. We find that β-VLDL and LDL are rapidly delivered to different endocytic compartments in these cells and that the two lipoproteins have markedly different rates of degradation.

Materials and Methods

Cells

Peritoneal macrophages were harvested from unstimulated male or female ICR mice (25–35 g; Harlan Sprague Dawley, Inc., Indianapolis, IN) as described (33) and plated onto polylysine-coated coverslip-bottom dishes (28) at a density of 5×10^4 cells per 10-mm coverslip for the fluorescence studies or onto 24-mm polylysine-coated tissue culture dishes (Corning Scientific Products, Corning, NY) (3×10^5 cells) for the protein degradation and CE hydrolysis studies. The cells were initially plated (day 0) into DME containing 10% (vol/vol) fetal bovine serum (HyClone Laboratories, Logan, UT), penicillin (100 U/ml), streptomycin (100 μg/ml), and glutamine (292 μg/ml), and maintained at 37°C in 8% CO_2/92% air. On day 1, the media was switched to DME containing 10% (vol/vol) lipoprotein-deficient serum (LPDS). Fresh DME/LPDS was added on day 2, and the experiments were performed on day 3.

Lipoproteins

The following lipoproteins were isolated by preparative ultracentrifugation: LDL (density, 1.020–1.063 g/ml) from fresh human plasma, LPDS (density, 1.215 g/ml) from fetal bovine serum, β-VLDL (density, 1.006 g/ml) from male New Zealand white rabbits (4 wk on a diet of rabbit chow [Purina] supplemented with 2% cholesterol/10% soybean oil [wt/wt], resulting in a plasma cholesterol of 3,300 mg/dl), and E2/E2 β-VLDL (density 1.006 g/ml; cholesterol and triglyceride = 218 and 590 mg/dl, respectively) from a male patient with familial dysbetalipoproteinemia (plasma cholesterol and triglyceride after 1 wk off niacin were 299 and 652 mg/dl, respectively; E2/E2 phenotype documented by isoelectric focusing [39] performed by Dr. Conrad Blum).

The LDL properties were as follows: mobility on 1% agarose electrophoresis = β; size by negative stain electron microscopy = 24 ± 1 nm with range = 22–26 nm (n = 50); composition (% by weight) = 30.2% protein, 7.9% free cholesterol, 67.7% cholesteryl ester, 8.5% triglyceride, and 30.2% phospholipid; and apoproteins appearing on 6% and 11% SDS-polyacrylamide electrophoresis = apo B-100.

The β-VLDL properties were as follows: mobility = mostly β with some material extending from the origin to the β region; size = 114 ± 50.3 nm with range = 66–280 nm (n = 100); composition = 1.1% protein, 3.6% free cholesterol; 55.4% cholesteryl ester; 33.3% triglyceride, and 6.6% phospholipid; and apoproteins = large and small apo B (approximately equal in proportion) and apo E.

The lipoproteins were fluorescently labeled by the method of Pitas et al. (27). Briefly, 200 μl of a 3 mg/ml solution of either DiI or DiO (Molecular Probes, Eugene, OR) in dimethyl sulfoxide was added to 4 mg (protein) of each lipoprotein in 8 ml of LPDS. After an 8-h incubation at 37°C, the labeled lipoproteins were reisolated by ultracentrifugation as described above.

The lipoproteins were labeled with ^{125}I (IMS.30; carrier-free; Amersham Corp., Arlington Heights, IL) using iodine monochloride as described previously (15). ^{125}I-LDL was 95% TCA precipitable, 95% chloroform inextractable, had a specific activity of 200–400 cpm/ng, and, by SDS-PAGE, had all of the label in apo B100. ^{125}I-β-VLDL was 95% TCA precipitable, 75–80% chloroform inextractable, had a specific activity of 200–400 cpm/ng, and, by SDS-PAGE, had most (~80%) of the label in apo E with the remainder equally divided between apo B100 and apo B48.

The lipoproteins were labeled with ^3H-CE as previously described (33). Briefly, semipurified cholesteryl ester transfer protein (kindly provided by Dr. Alan Tall, Columbia University, New York) was used to transfer ^3H-CE from ^3H-CE-labeled HDL to either LDL or β-VLDL. The ^3H-CE-labeled HDL donor was made by injecting human plasma with 7-^3H(N)-cholesterol (30 Ci/mmol, New England Nuclear, Cambridge, MA), allowing lecithin/cholesterol acyl transferase to esterify the cholesterol, reisolating the labeled HDL, and depleting the labeled HDL of any residual free ^3H-cholesterol by incubation with lower density lipoproteins. 99% of the radioactivity in the labeled LDL and β-VLDL was in the cholesterol moiety of CE (with 1% in free cholesterol). The specific activities of ^3H-CE-labeled LDL and β-VLDL were, respectively, 0.92 and 1.52 cpm/pmol CE.

All radioactively labeled lipoproteins were used within 3 wk of the labeling procedure.

Video Intensification Fluorescence Microscopy

Cells were incubated at 37°C in a heating box (no CO_2) with the labeled lipoproteins in DME without bicarbonate containing 0.2% (wt/vol) fatty acid-free BSA (Sigma Chemical Co., St. Louis, MO) and 10 mM Hepes, pH 7.4 (medium A), according to the individual figure legends. At the end of the incubation, the cells were quickly washed three times with PBS and either viewed immediately or fixed with 2% formaldehyde in PBS, and then placed in PBS for viewing. Fluorescence images were obtained using a Leitz Diavert microscope with a 63×, NA 1.4 objective. For observation of DiI fluorescence, a "rhodamine" filter set was used (530–560-nm excitation filter, 580-nm dichroic, and 580-nm long pass filter). For DiO fluorescence, a "fluorescein" filter set was used (450–490 nm excitation, 510-nm dichroic, and 515-nm long pass filter). In some cases, a 520-nm bandpass emission filter was used to make sure that DiI fluorescence did not pass through the DiO filter set. Images were recorded with a Videoscope (Washington, DC) KS 1381 image intensifier, a VS 2000N video camera, and a JVC 6650U videocassette recorder. Images were digitized with a Gould IP 8400 image processor, and photographs were produced with a Polaroid Freeze Frame.

Electron Microscopy

DiI was converted to an electron-dense stain by photobleaching in the presence of DAB using a procedure adapted from Sandell and Masland (29) and Godement et al. (12). Cells grown on 35-mm tissue culture dishes (Falcon Labware, Oxnard, CA) were incubated with medium A containing 10 μg/ml DiI-β-VLDL or 100 μg/ml DiI-LDL for 10 min at 37°C, rinsed, and fixed with 2.5% paraformaldehyde/0.5% glutaraldehyde in PBS for 10 min at room temperature. The cells were rinsed and placed in 0.1 M Tris-HCl (pH 8.2) containing 1.5 mg/ml DAB (filtered through a 0.2-μm filter). A region ~2 mm in diameter was bleached for 40 min using an upright Nikon microscope with a 100 W Hg arc lamp, a 10× (NA 0.5) Fluor objective, and a rhodamine filter set. The cells were then rinsed, fixed in 2.5% glutaraldehyde, and stained with 1% OsO_4 in 0.1 M phosphate buffer for 30 min. The samples were dehydrated in graded ethanol washes and embedded in Epox (Ernest F. Fullam, Inc., Latham, NY), keeping track of the photobleached region. Thin sections were observed without further staining to facilitate observation of the DAB reaction product. Photographs were taken at 20,000× using a JEOL 100S electron microscope. Control cells were processed identically except that labeled lipoproteins were omitted from the initial incubation.

^{125}I-labeled Lipoprotein Degradation and Internalization Assay

Cell monolayers in 24-mm dishes were pulse labeled with the ^{125}I-labeled lipoproteins (in the absence or presence of 50-fold excess unlabeled lipoproteins) for 10 min at 37°C in a heating box (no CO_2) in 0.5 ml medium A (no bicarbonate). The monolayers were then washed three times rapidly with warm medium A and then incubated in the heating box for the indicated chase times in 1 ml medium A. At the end of the chase period, the cells

were rapidly chilled on ice, the media was harvested (for the degradation assay), and the monolayers were washed three times with ice-cold PBS. The monolayers were then incubated for 1 h at 4°C on a rocking platform with 1 ml of buffer containing 10 mM suramin (Mobay Chemical Corp., Pittsburgh, PA), 50 mM NaCl, 3 mM $CaCl_2$, and 10 mM Hepes, pH 7.4, to help differentiate surface-bound from internalized lipoprotein (7). In a control experiment in which macrophages were incubated with the two labeled lipoproteins at 4°C (to prevent internalization), we found that suramin releases 75% of surface-bound LDL and 60% of surface-bound β-VLDL. The monolayer was then dissolved in 1 ml of 0.1 N NaOH and analyzed for radioactivity and protein content. The media was assayed for TCA-soluble, chloroform nonextractable cpm ("degraded" lipoprotein) as previously described (15).

^{125}I-α_2-macroglobulin Degradation and Cell Association Assay

α_2-macroglobulin was purified, converted to the receptor-binding form, and iodinated as previously described (28). Cell monolayers were incubated with ^{125}I-α_2-macroglobulin as described in the legend to Fig. 9. The media was assayed for ^{125}I-α_2-macroglobulin degradation exactly as described above for ^{125}I-lipoprotein degradation. Cell association was determined by counting an aliquot of the 0.1 N NaOH cell digest.

Lipoprotein CE Hydrolysis Assay

Cell monolayers (24 mm) were preincubated for 30 min in medium A in the absence or presence of 5 μg/ml Sandoz ACAT-inhibitor 58-035 (kindly provided by Dr. John Heider, Sandoz, Inc., East Hanover, NJ) as described previously (36). The cells were then pulsed (10 min) and chased (20 min) with ^{3}H-CE-labeled LDL or β-VLDL exactly as described above for the ^{125}I-labeled lipoprotein experiments except that the pulse and chase media of the ACAT-inhibited cells (i.e., cells preincubated with 58–035) contained 5 μg/ml 58–035. At the end of the experiment, the cells were rapidly chilled on ice, the media was removed, and the monolayers were washed three times with ice-cold PBS. The cells were then lipid extracted in situ with 1 ml 3:2 (vol/vol) hexane/isopropanol (1 h, room temperature). The lipid extract was then fractionated by thin layer chromatography and the radioactivity in free cholesterol and CE was determined as previously described (36).

Other Assays and Procedures

Whole-cell ACAT activity was measured in living cell monolayers by the ^{14}C-oleate pulse method (33). Protein was measured by the method of Lowry et al. (23); fluorescently labeled lipoproteins were delipidated by 3/2 (vol/vol) hexane/isopropanol extraction before protein measurement. Total lipoprotein cholesterol content was measured by gas-liquid chromatography of alkaline hydrolysates of the lipoprotein lipid extracts as previously described (33).

Results

Characterization of Fluorescently Labeled Lipoproteins

To trace the endocytic pathways of LDL and β-VLDL by fluorescence microscopy, the particles were labeled with one of two fluorescent lipid analogues—DiI and DiO. DiI is an ideal label since, once incorporated into the lipoprotein, it does not readily diffuse out of the particle (26). In a few double-label experiments described below, DiO-labeled lipoproteins were also used. DiO is structurally similar to DiI and, like DiI, is readily and stably incorporated into lipoproteins. All of the labeled lipoproteins had similar cholesterol/protein ratios to the respective unlabeled lipoproteins from which they were derived (data not shown). In addition, the fluorescently labeled lipoproteins behaved like their ^{125}I-labeled counterparts in cellular uptake competition assays (9, 21): DiI-β-VLDL uptake was competed by excess unlabeled β-VLDL (100-fold excess) and LDL (1,000-fold excess) but not by acetyl-LDL (1,000-fold excess), and DiI-LDL uptake

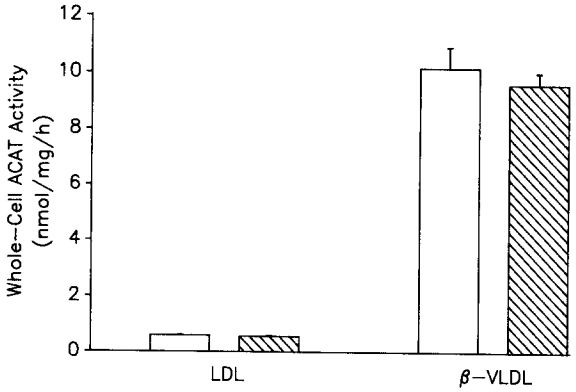

Figure 1. Stimulation of ACAT in mouse peritoneal macrophages by unlabeled and DiI-labeled LDL and β-VLDL. Macrophages were incubated for 7 h with DMEM/10% LPDS containing unlabeled (*open bars*) or DiI-labeled (*hatched bars*) LDL (20 μg protein/ml, 50 μg cholesterol/ml) or β-VLDL (3.3 μg protein/ml, 50 μg cholesterol/ml). During the last 2 h of the 7-h incubation, the cells were incubated with ^{14}C-oleate-albumin complex. At the end of the 7-h incubation, the cells were assayed for cholesteryl ^{14}C-oleate content ("whole-cell ACAT activity") as described (28). Values shown are means ± SEM (n = 3).

was also competed by excess unlabeled LDL (100-fold excess) and β-VLDL (50-fold excess) but not by acetyl-LDL (100-fold excess) (data not shown). Furthermore, both labeled LDL and β-VLDL uptake were markedly reduced in macrophages which had been cholesterol-loaded to down-regulate the LDL receptor (see below). Lastly, the respective labeled and unlabeled lipoproteins had similar ACAT-stimulatory potential in macrophages. The data in Fig. 1 show that DiI-labeled LDL and β-VLDL (*hatched bars*) stimulated macrophage ACAT to the same level as the respective unlabeled lipoproteins (*open bars*). The data in Fig. 1 also serve to reemphasize the point that β-VLDL is a much more potent stimulator of macrophage ACAT than LDL. (Subsequent work in our laboratory has disclosed that the greater ACAT-stimulatory potential of β-VLDL is not due to greater delivery to the cell of β-VLDL-CE-derived free cholesterol; see below and Discussion.) Thus, the fluorescently labeled lipoproteins used in this study had similar cell uptake properties (consistent with the hypothesis that LDL and β-VLDL bind to the same receptor in macrophages [9, 21]) and ACAT-stimulatory properties (in which β-VLDL is more potent than LDL) to the respective unlabeled lipoproteins.

Video Intensification Fluorescence Microscopy of Endocytosed LDL and β-VLDL in Mouse Peritoneal Macrophages

Macrophages were incubated with DiI-LDL or DiI-β-VLDL for 10 min at 37°C (Fig. 2). Fig. 2 *A* shows the LDL pattern: fluorescence concentrated near the center of the cell consisting of either a few bright vesicles or a diffuse pattern. A few more widely distributed vesicles were also seen. In contrast, the β-VLDL pattern (Fig. 2 *B*) consisted predominantly of distinct, bright vesicles seen throughout the cytoplasm. Little or no fluorescence was apparent with either lipoprotein (Fig. 2 *C* for DiI-LDL and Fig. 2 *D* for DiI-β-VLDL) when the same experiment was performed using macrophages that had been extensively loaded with cholesterol (by a 48-h

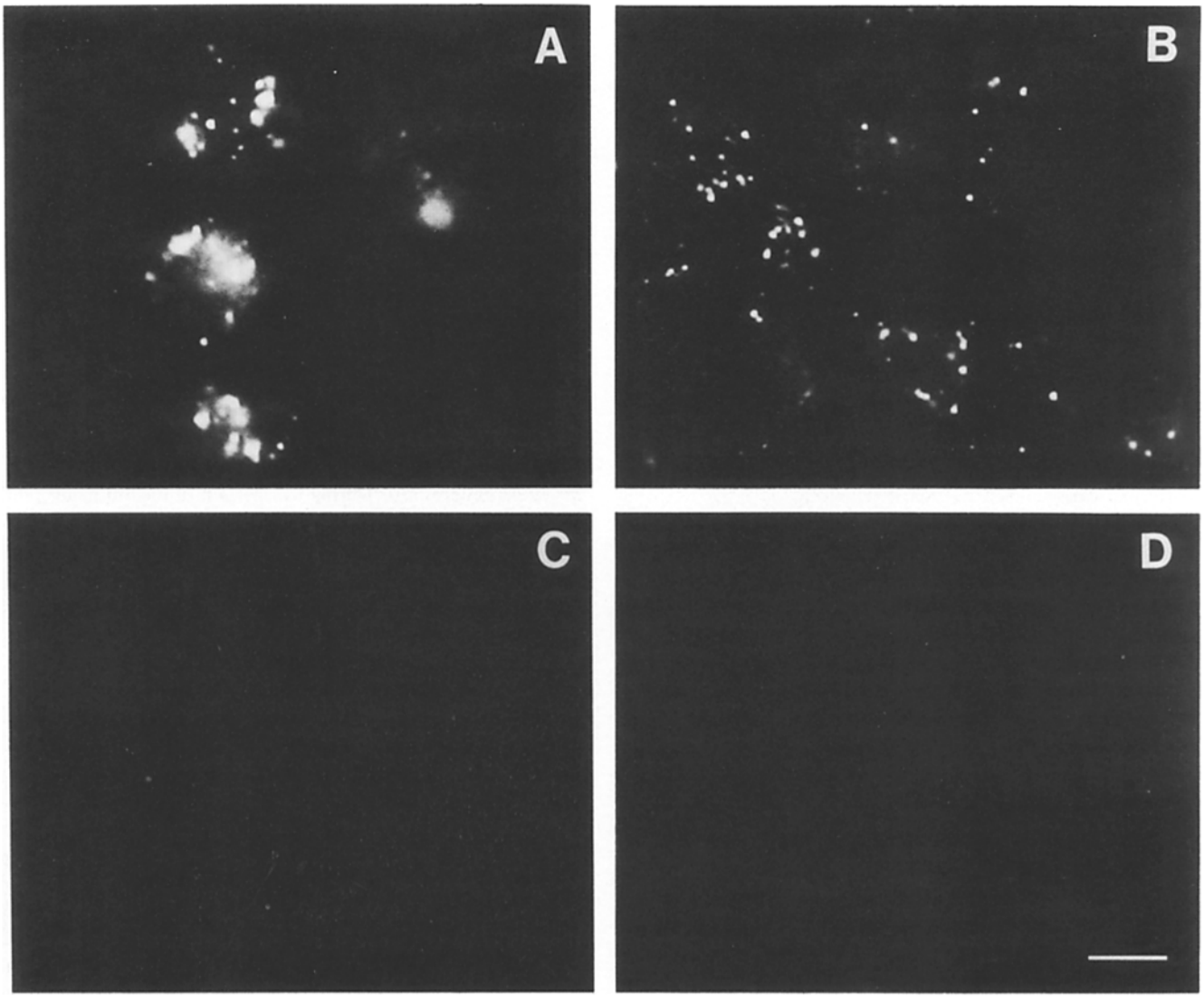

Figure 2. Fluorescence microscopy of macrophages incubated 10 min with DiI-labeled LDL and β-VLDL. Macrophages were incubated with medium A containing DiI-LDL (20 μg protein/ml) (*A*) or with DiI-β-VLDL (5 μg protein/ml) (*B*) for 10 min at 37°C and then viewed (after fixation) by video intensification fluorescence microscopy. In *C* (DiI-LDL) and *D* (DiI-β-VLDL), the same incubations were performed using cells which had been preincubated for 48 h with DME/10% fetal bovine serum containing 50 μg protein/ml acetyl-LDL. Bar, 10 μm.

preincubation with acetylated LDL) to effect downregulation of the cells' LDL receptors (14).

To compare the endocytic pattern of LDL vs. β-VLDL in the same cell, we conducted a double-label experiment in which DiO-LDL plus DiI-β-VLDL were incubated with macrophages for 10 min at 37°C (Fig. 3, *A* [LDL pattern] and *B* [β-VLDL pattern]). Note that the same field of cells in the same orientation (photographed a few seconds apart using different filters) is shown in Fig. 3, *A* and *B*. The LDL pattern (Fig. 3 *A*) in this experiment was, as in Fig. 2 *A*, predominantly central, although not as diffuse as the pattern in Fig. 2 *A*. The β-VLDL pattern (Fig. 3 *B*) in this experiment consisted of both central vesicles and vesicles distributed throughout the cytoplasm. (Although the outlines of the individual cells are difficult to see, the bright dots seen outside the central areas of the cells in Fig. 3 *B* are all within the boundaries of the cells' peripheries.) In several of the cells, there was some overlap (as well as some differences) when one compares just the central vesicles of each lipoprotein pattern. The vesicles seen outside the central region, however, were a feature seen almost exclusively with β-VLDL. The same experiment done with the labels switched (i.e., DiI-LDL plus DiO-β-VLDL) is shown in Fig. 3, *C* (LDL) and *D* (β-VLDL). As above, the LDL pattern (Fig. 3 *C*) was mostly central, whereas the β-VLDL pattern (*D*) consisted of vesicles seen throughout the cell. Thus, in both single-label and double-label experiments, LDL and β-VLDL gave different cellular patterns of fluorescence in macrophages after 10 min of continuous uptake.

To determine the time course of the differences between the LDL and β-VLDL patterns, cells were incubated ("pulsed") with DiI-LDL or DiI-β-VLDL for 2 min and then incubated in the absence of lipoproteins ("chased") for various times (Fig. 4). Even after a 2-min pulse, there was a distinct differ-

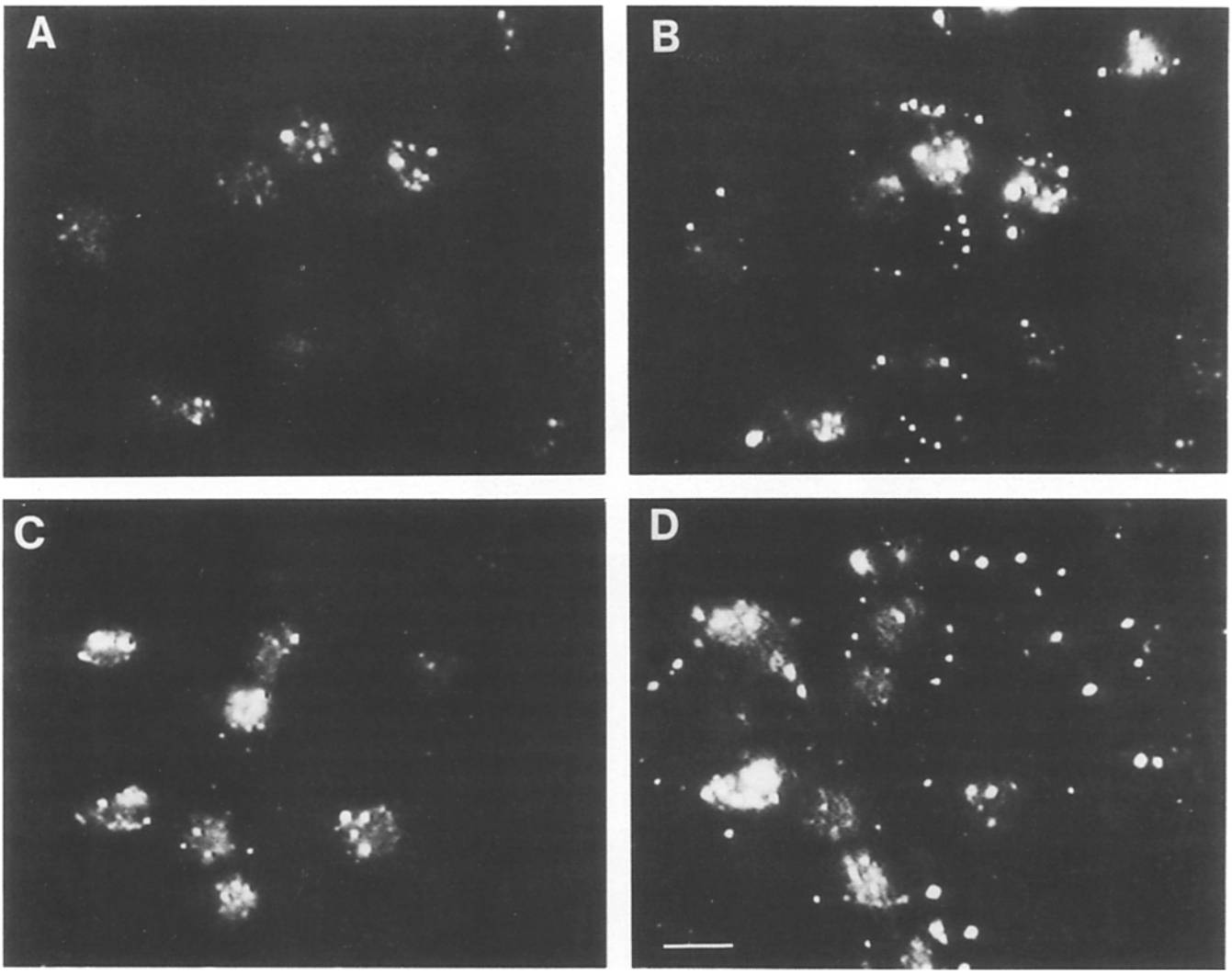

Figure 3. Double-label fluorescence microscopy of macrophages incubated 10 min with DiI and DiO-labeled LDL and β-VLDL. Macrophages were incubated with medium A containing DiO-LDL (50 μg protein/ml) plus DiI-β-VLDL (2 μg protein/ml) for 10 min at 37°C and then viewed (without fixation) by fluorescence microscopy to visualize either DiO (LDL) (*A*) or DiI (β-VLDL) (*B*). A similar experiment was performed using DiI-LDL (50 μg protein/ml) plus DiI-β-VLDL (5 μg protein/ml): the DiI (LDL) and DiO (β-VLDL) patterns are shown in *C* and *D*, respectively. Bar, 10 μm.

ence between the two lipoproteins: the LDL pattern (Fig. 4 *A*) consisted of fluorescent dots of various degrees of brightness throughout the cell with a diffuse haze (probably small vesicles out of focus) in the central region. In contrast, the β-VLDL pattern (Fig. 4 *G*) consisted of fewer, brighter, and more peripheral dots which may have been at or near the cell surface. After a 2-min chase, the LDL pattern (Fig. 4 *B*) evolved into one consisting primarily of central vesicles of increased intensity; the β-VLDL pattern (Fig. 4 *H*) still showed fluorescence extending out to the edge of the cell without central vesicles. By 5 min, the LDL pattern (Fig. 4 *C*) was clearly established as intense, central fluorescence, whereas the β-VLDL pattern (Fig. 4 *I*) was widely-distributed without central fluorescence. At 10 min, the LDL pattern (Fig. 4 *D*) showed bright, central fluorescence without resolvable discrete vesicles; the β-VLDL pattern (Fig. 4 *J*) evolved somewhat in that a central, diffuse fluorescence was now apparent, but discrete dots outside the central region were still quite prevalent. At 15 and 20 min of chase, the LDL pattern (Fig. 4, *E* and *F*, respectively) showed a diffuse, less centralized pattern of fluorescence which might have been the result of breakdown of the LDL. The β-VLDL pattern at 15 and 20 min (Fig. 4, *K* and *L*, respectively) also showed some diffuse haze, although even at these late time points, discrete central and more widely-distributed dots were seen. Thus, the patterns of LDL and β-VLDL endocytosis in mouse peritoneal macrophages appeared to be different as early as 2 min of incubation and remained clearly distinguishable after 10 min of chase time.

Since the patterns of LDL and β-VLDL were distinguishable after 2 min of incubation at 37°C (Fig. 4, *A* and *G*, respectively), we next sought to compare the cell surface binding pattern of the two lipoproteins. DiO-labeled LDL and DiI-labeled β-VLDL were coincubated with cells for 2 h at 4°C (at which temperature there is no endocytosis) (Fig. 5). Both β-VLDL (Fig. 5 *A*) and LDL (Fig. 5 *B*) showed a pattern of fluorescent dots around the perimeter of the cell consistent with cell surface binding. In some regions where

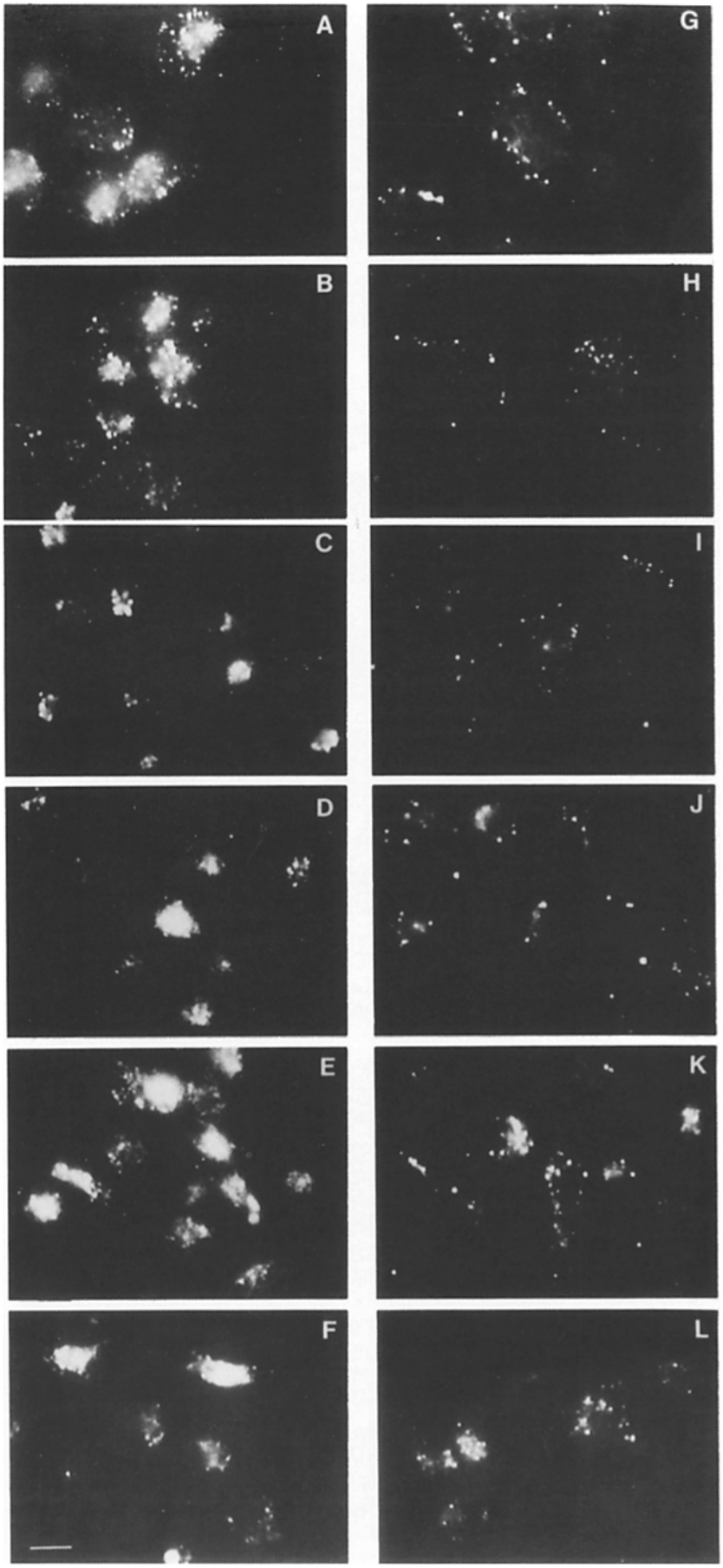

Figure 4. Time course of fluorescence microscopic pattern of macrophages incubated with DiI-labeled LDL and β-VLDL. Macrophages were incubated with medium A containing 20 μg protein/ml DiL-LDL (*A–F*) or 5 μg protein/ml DiI-β-VLDL (*G–L*) for 2 min at 37°C. The cells were then either fixed and viewed by fluorescence microscopy (*A* and *G*) or chased in medium A without lipoproteins for 2 (*B* and *H*), 5 (*C* and *I*), 10 (*D* and *J*), 15 (*E* and *K*), or 20 min (*F* and *L*), and then fixed and viewed. Bar, 10 μm.

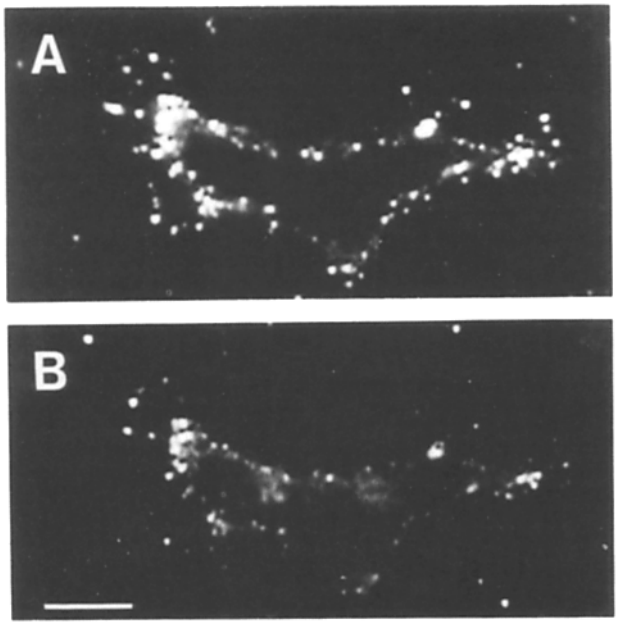

Figure 5. Fluorescence microscopy of macrophages incubated with DiO-labeled LDL and DiI-labeled β-VLDL at 4°C. Macrophages were incubated with medium A containing 200 μg protein/ml DiO-LDL and 1 μg protein/ml DiI-β-VLDL for 2 h at 4°C. After fixation for 1 h at 4°C, the cells were viewed by fluorescence microscopy to visualize either DiI (β-VLDL) (*A*) or DiO (LDL) (*B*). Bar, 10 μm.

the cells have spread thinly over the substratum, patterns of cell surface fluorescent dots could be resolved. Although there are some differences, it is clear that the overall cell surface distribution of the two lipoproteins was similar. Thus, the marked differences in cellular distribution of LDL vs. β-VLDL seen after incubation at 37°C (above) most likely reflected differences related to early endocytosis rather than differences of distribution of cell surface binding of the two lipoproteins.

Electron Microscopy of DiI-β-VLDL-containing Vesicles in Mouse Peritoneal Macrophages

The fluorescence microscopy studies described above indicated that the major difference in the endocytic patterns of LDL and β-VLDL in mouse peritoneal macrophages was that β-VLDL, but not LDL, was targeted to a set of peripheral vesicles. To examine these β-VLDL-containing vesicles at the ultrastructural level, we used a technique whereby the DiI could be converted into an electron-dense marker (12, 29). Cells were incubated with DiI-labeled β-VLDL for 10 min at 37°C and then fixed. The cells were then photobleached on a microscope in the presence of DAB. Visualization of the DAB reaction product is enhanced by OsO_4 staining.

The electron micrographs in Fig. 6, *A* and *B* show the appearance of vesicles marked by electron-dense staining in cells incubated with DiI-β-VLDL. The vesicles, which were 300–600 nm in diameter and distributed widely throughout the cytoplasm, were distinguished by the appearance of dark staining around the periphery of the vesicle. In some vesicles, there was also electron-dense material (sometimes roughly spherical) attached to the inner surface of the vesicle membrane but the vesicle interior was otherwise relatively electronlucent. Vesicles with this type of appearance were prominent only in cells incubated with DiI-β-VLDL and not in cells incubated with either DiI-LDL or incubated in the absence of lipoproteins. The identification of vesicles containing DiI-LDL was more difficult by this technique. In the cells incubated with DiI-LDL, there were vesicles (200–600 nm in diameter), apparently stained with electron-dense material, that appeared to have an electron-dense "background" and resembled "multivesicular bodies" or lysosomes (not shown). However, similar structures also contained electron-dense material in cells incubated without DiI-LDL. As described below, the kinetics of degradation indicate that LDL is rapidly delivered to lysosomes. This photobleaching

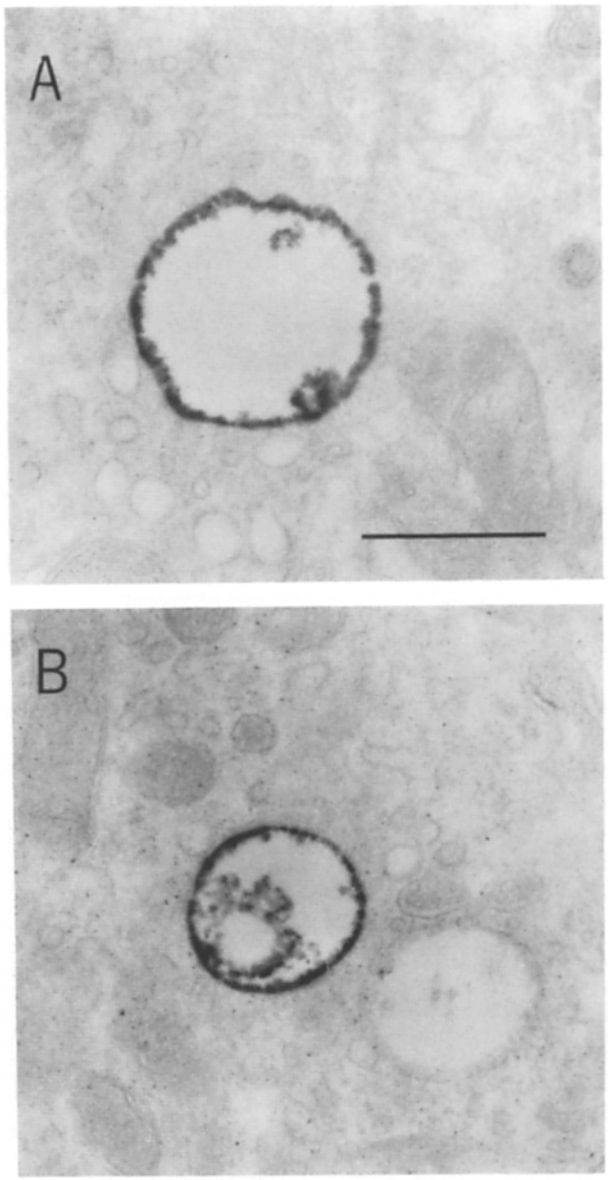

Figure 6. Electron microscopy of macrophages incubated with DiI-β-VLDL and processed using DAB. Macrophages were incubated with medium A containing 5 μg protein/ml DiI-β-VLDL for 10 min at 37°C and then fixed and processed for electron microscopy using DAB as described in Materials and Methods. *A* and *B* are photographs of vesicles from two different cells. Bar, 0.5 μm.

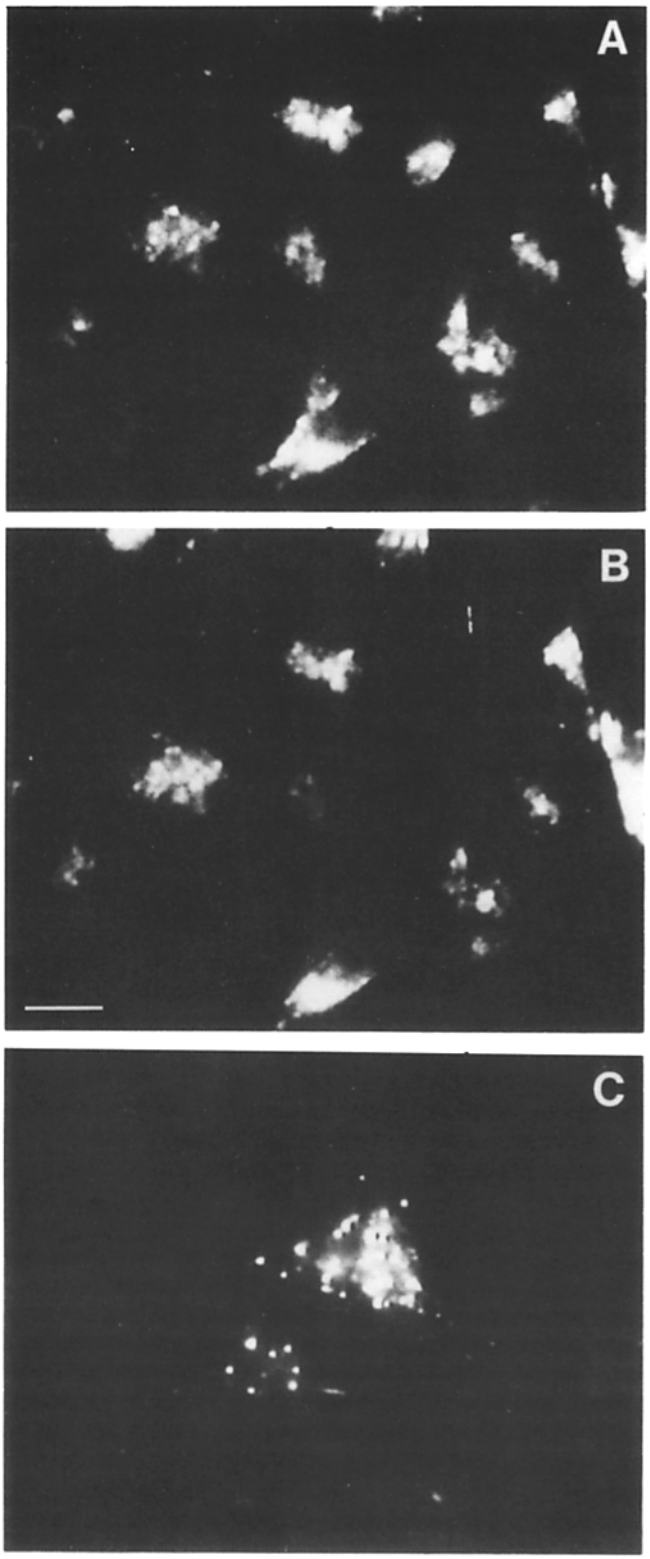

Figure 7. Fluorescence microscopy of macrophages incubated with DiO-LDL plus DiI-E2-β-VLDL. (*A* and *B*) A macrophage monolayer was incubated with medium A containing DiO-LDL (20 μg protein/ml) plus DiI-E2-β-VLDL (20 μg protein/ml) for 5 min and then chased in the absence of lipoproteins for 15 min. The cells were then fixed and viewed for DiO (LDL) fluorescence (*A*) and DiI (E2-β-VLDL) fluorescence (*B*). (*C*) Another macrophage monolayer was incubated with medium A containing DiI-β-VLDL (5 μg protein/ml) for 5 min and then chased for 15 min. The cells were then fixed and viewed. Bar, 10 μm.

procedure may not provide a dark enough stain to be observed reliably over the background in lysosomes.

Thus, consistent with the fluorescence microscopy data showing targeting of fluorescently labeled β-VLDL to a set of widely distributed vesicles not seen with labeled LDL, the electron micrographic study described above demonstrated a set of vesicles with electron-dense markings prominent only in cells incubated with DiI-β-VLDL.

Fluorescence Pattern of E2-β-VLDL in Mouse Peritoneal Macrophages

The difference in distribution of LDL and β-VLDL-containing vesicles in mouse peritoneal macrophages may be related to the fact that β-VLDL binds to its macrophage receptor with much greater affinity than LDL (9, 21). Therefore, we examined the pattern of endocytosis of E2-β-VLDL, a form of β-VLDL which, by virtue of a single amino acid substitution in the receptor-binding region of its apo E, binds to its receptor with a very low affinity (18); thus, its binding affinity to the mouse peritoneal macrophage surface is more similar to that of human LDL than to that of hypercholesterolemic rabbit β-VLDL (9, 21). Also, the ACAT-stimulatory ability of E2-β-VLDL is more similar to that of LDL than that of hypercholesterolemic β-VLDL (reference 19 and verified by us).

Fig. 7, *A* and *B* show the results of a double-label experiment in which a monolayer of macrophages was pulsed for 5 min with DiO-LDL (visualized in *A*) plus DiI-E2-β-VLDL (*B*) and then chased for 15 min. For comparison, *C* in Fig. 6 shows a 5-min pulse/15-min chase (in another monolayer of cells) with DiI-β-VLDL. The LDL and E2-β-VLDL patterns appeared virtually identical to each other and distinct from the β-VLDL pattern. Thus, E2-β-VLDL, a lipoprotein with a receptor-binding affinity and an ACAT-stimulatory potential much more similar to those of LDL than to those of hypercholesterolemic β-VLDL, was associated with a pattern of endocytosis which was also more similar to that of LDL than to that of β-VLDL.

Time Course of LDL and β-VLDL Protein Degradation and Cholesteryl Ester Hydrolysis in Mouse Peritoneal Macrophages

Given the endocytic divergence of LDL and β-VLDL in mouse peritoneal macrophages (above), we next sought to determine if there were differences in the rate or extent of protein degradation and CE hydrolysis of the two lipoproteins. For the protein degradation study, ^{125}I-labeled LDL or β-VLDL were incubated with cells for 10 min, and then the cells were chased in the absence of lipoproteins for 5–30 min thereafter. As shown in Fig. 8 *A*, the degradation of ^{125}I-labeled LDL to TCA-soluble material was rapid and extensive (70% of total cpm at 20 min). In contrast, the conversion of ^{125}I-β-VLDL to TCA-soluble material occurred at a slower, continuous pace over the 30-min chase period, reaching only 37% (of total cpm) at 30 min (Fig. 8 *B*). Note that the slower degradation of ^{125}I-β-VLDL could not be explained by a slower rate of β-VLDL internalization. Firstly, very little labeled β-VLDL is suramin releasable (Fig. 8 *B*), indicating a relatively small amount of surface-bound material even when one factors in the finding that the suramin-releasable material may represent 60% of the true surface-bound material (see Materials and Methods). Secondly, we

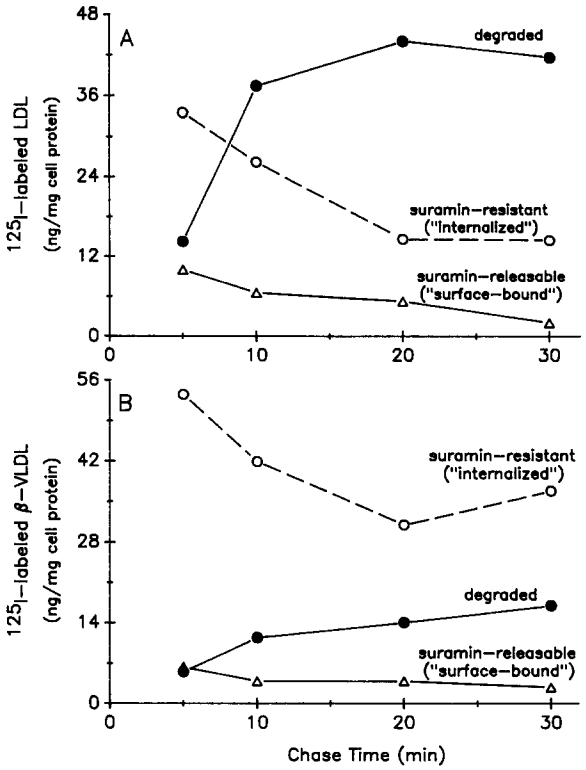

Figure 8. Time course of degradation of ^{125}I-labeled LDL and β-VLDL in mouse peritoneal macrophages. Macrophages were incubated with medium A containing 20 μg/ml ^{125}I-labeled LDL (*A*) or 2 μg/ml β-VLDL (*B*) in the presence or absence of 50-fold excess unlabeled lipoprotein for 10 min at 37°C. The cells were then washed and chased in medium A alone for the indicated times. The media were assayed for ^{125}I-lipoprotein degradation (*solid circles*) and the cells were assayed for suramin-resistant (*open circles*) and suramin-releasable (*open triangles*) ^{125}I-lipoproteins as described in Materials and Methods. See Results and Materials and Methods for a description of how suramin-resistant and releasable material approximates internalized and surface-bound lipoproteins, respectively. All of the suramin-resistant ("internalized") ^{125}I radioactivity was TCA precipitable. Each value shown (specific value) was derived by subtracting the value in the presence of unlabeled lipoprotein (nonspecific value) from the value in the absence of unlabeled lipoprotein (total value). The nonspecific value was never more than 10% of the total value. All values shown are average of duplicate values, which varied by <10%. The media were also assayed for TCA-precipitable material to detect the possible occurrence of lipoprotein recycling. Although there was some TCA-precipitable material in the media of both the LDL and β-VLDL cells (maximum = 20% total cpm at 20 min with both lipoproteins), it is not known what percentage of this material actually entered the cells and whether the material contained intact apoproteins or was lipid-associated (too few cpm to analyze).

have demonstrated morphological evidence of rapid internalization of DiI-β-VLDL in Fig. 4. Thus, both LDL and β-VLDL both rapidly entered the macrophages, but the β-VLDL was degraded (to TCA-soluble material) at a much slower rate.

To compare the degradation of LDL and β-VLDL with a nonlipoprotein ligand internalized by macrophages via receptor-mediated endocytosis, α_2-macroglobulin (38), we assayed the specific degradation and cell association of ^{125}I-α_2-macroglobulin after a 10-min pulse and 30-min chase (Fig. 9, *Control*). Similar to the case with LDL, 88% of the ^{125}I-α_2-macroglobulin was degraded after 30 min. To determine if the relatively slow degradation of β-VLDL might be caused by some general inhibitory effect of this lipoprotein on degradation of endocytosed ligands, ^{125}I-α_2-macroglobulin was coincubated with unlabeled β-VLDL during the 10-min pulse period and then chased and assayed for degradation and cell association as above (Fig. 9, *Plus β-VLDL*). Although the amount of ^{125}I-α_2-macroglobulin internalized by the cell was slightly less under these conditions, the ^{125}I-α_2-macroglobulin was still extensively (93%) degraded. Thus, both LDL and α_2-macroglobulin in contrast to β-VLDL, were both extensively and rapidly degraded by mouse peritoneal macrophages. Furthermore, it is unlikely that the relatively slower degradation of β-VLDL could be explained by general inhibition by this lipoprotein of intracellular degradation of endocytosed ligands.

We next examined the hydrolysis of the cholesteryl esters of LDL and β-VLDL. The two lipoproteins were labeled with ^{3}H-CE using CE transfer protein (as described in Materials and Methods) such that 99% of the ^{3}H-cpm were in the cholesterol moiety of CE (with 1% in free cholesterol). Cells were pulse labeled with ^{3}H-CE-LDL or β-VLDL for 10 min and then chased in the absence of lipoproteins for 20 min. The cells (and the media) were then assayed for the presence of ^{3}H-CE (i.e., unhydrolyzed material) and [^{3}H]cholesterol (i.e., hydrolyzed material). The incubations were done in the presence of the ACAT inhibitor, Sandoz compound 58-035, to prevent any hydrolyzed lipoprotein-derived [^{3}H]cholesterol from being reesterified back to ^{3}H-CE by ACAT. The data in Fig. 10 show that, by 20 min of chase time, the cholesteryl esters of LDL were almost completely (95%) hydrolyzed. In contrast, only 27% of the cholesteryl esters of β-VLDL were hydrolyzed in this same time period.

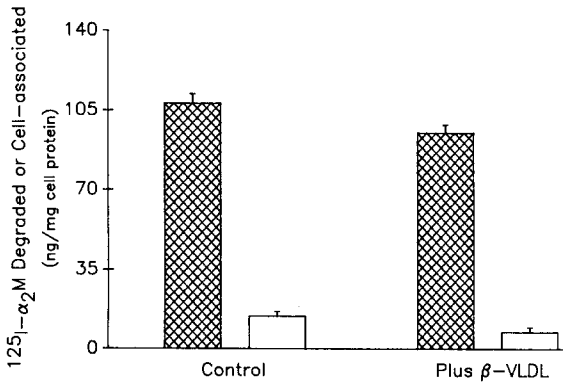

Figure 9. Specific degradation and cell association of ^{125}I-α_2-M (^{125}I-α_2-macroglobulin) in mouse peritoneal macrophages. Macrophages were incubated with medium A containing 10 μg/ml ^{125}I-α_2M in the absence or presence of unlabeled α_2M (1 mg/ml) for 10 min at 37°C. The incubation media for certain cells also contained unlabeled β-VLDL (2 μg/ml) (*Plus β-VLDL*). The cells were then washed and chased in medium A alone for 30 min at 37°C. The chase media were assayed for degraded ^{125}I-α_2M (*hatched bars*), and the remaining cell-associated ^{125}I-α_2M (*open bars*) was determined as described in Materials and Methods. Each value shown (specific value) was derived by subtracting the value in the presence of unlabeled α_2M (nonspecific value) from the value in the absence of unlabeled α_2M (total value). The nonspecific value was never more than 5% of the total value. Values shown are means ± SEM (n = 3).

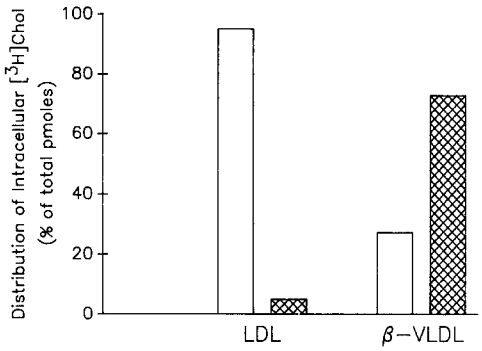

Figure 10. CE hydrolysis of ^{3}H-CE-labeled LDL and β-VLDL in ACAT-inhibited mouse peritoneal macrophages. Macrophages were preincubated for 30 min in medium A containing 5 μg/ml 58-035 and then incubated for 10 min in medium A containing 58-035 plus 100 μg CE/ml ^{3}H-labeled LDL (0.92 cpm/pmol CE) or β-VLDL (1.52 cpm/pmol CE). The cells were then washed and chased for 20 min in medium A containing 5 μg/ml 58-035. All incubations were at 37°C. Lipid extracts of the cells were then assayed for ^{3}H-labeled free cholesterol (*open bars*) and CE (*hatched bars*) by thin layer chromatography as described in Materials and Methods. The values shown are percentages of total cellular [^{3}H]cholesterol; 100% values for LDL and β-VLDL were 586 and 1,082 pmol/mg cell protein, respectively. Each value shown is the average of duplicate values, which differed by <10%. The chase media from these incubations contained no detectable radioactivity.

There were no ^{3}H-cpm in the media. Furthermore, the results of this experiment were essentially the same (94% hydrolysis of LDL-CE and 32% hydrolysis of β-VLDL-CE) when done in the absence of the ACAT inhibitor (indicating that [*a*] ACAT had not yet esterified the newly hydrolyzed lipoprotein cholesterol; and [*b*] the ACAT inhibitor did not introduce an artefact into the experiment). Thus, in comparison with LDL, the hydrolysis of β-VLDL CE, like the degradation of β-VLDL protein, was markedly diminished in mouse peritoneal macrophages.

Discussion

The data presented here describe morphological and biochemical differences in the pattern of endocytosis of LDL and β-VLDL in mouse peritoneal macrophages. These differences are quite striking when one considers previous studies on the endocytosis of different ligands. For instance, Maxfield et al. (25), using double-label fluorescence microscopy, have shown that insulin, EGF, and α_2-macroglobulin, each of which bind to different receptors, are internalized within the same vesicles in 3T3 cells. Similarly, Ward et al. (38), using a density shift technique, have demonstrated the presence of common early endosomes containing α_2-macroglobulin, mannose-terminal proteins, transferrin, and maleylated proteins in rabbit alveolar macrophages. In addition, several groups have shown in nonmacrophage cells that LDL is internalized into the same early endosome as other ligands, including EGF and transferrin in HeLa cells (1) and EGF (6) and α_2-macroglobulin (37) in human fibroblasts. Furthermore, Jaeckle et al. (20) have reported that LDL and β-VLDL appear in similar endosomal subfractions of rat liver homogenates 15 min after intravenous injection of the lipoproteins into the animals.

Distinct localization of endocytosed ligands clearly does occur in other cases. For example, transferrin is separated from degraded ligands (e.g., LDL) because the transferrin remains bound to its receptor as it recycles back to the cell surface (16). In polarized epithelial cells, some internalized ligands are degraded while others are transported by vesicles across the cell (16). In this light, our finding that β-VLDL protein degradation and CE hydrolysis are markedly retarded (compared to that of LDL and, in the case of protein degradation, to that of α_2-macroglobulin) in mouse peritoneal macrophages (Figs. 7 and 8) may indicate that the β-VLDL-containing vesicles represent another type of non-degradative or slowly degradative vesicles. It is also interesting to note that electron micrographs of some horseradish peroxidase–containing vesicles (stained with DAB) in mouse peritoneal macrophages (31) appear very similar to our electron micrographs of β-VLDL-containing vesicles in these cells (Fig. 6). Further identification of the β-VLDL-containing vesicles must await additional work in this area.

Given the differences in both endocytic targeting and kinetics of degradation of LDL and β-VLDL, the most likely interpretation is that the β-VLDL-containing vesicles might contain less or different degradative enzymes (or a different environment, like a higher pH) than the LDL-containing vesicles, which have the morphological and kinetic properties of lysosomes. It is theoretically possible that the biochemical differences might partially reflect the different properties of the substrates (and hence their possible different susceptibilities to degradation). For instance, the ^{125}I-labeled protein in LDL is apo B whereas the major labeled protein in β-VLDL was apo E (see Materials and Methods). Regarding the CE substrates, β-VLDL (60–280 nm) is a bigger particle than LDL (22–26 nm), and thus access to the CE core by the CE hydrolase might influence the rate of CE hydrolysis. However, it is unlikely that the marked differences demonstrated here between LDL and β-VLDL protein degradation and CE hydrolysis could be entirely explained by these substrate differences.

What could be the possible mechanism(s) involved in the different patterns of endocytosis of LDL vs. β-VLDL? One possibility would be that the differences are related to the two lipoproteins binding to different cell surface receptors. For instance, Kowal et al. (22) have recently identified a protein other than the LDL receptor (termed LDL receptor-related protein or "LRP") which mediates the endocytosis of apo E–enriched β-VLDL in human fibroblasts. However, the following points suggest that the uptake of DiI-β-VLDL by mouse peritoneal macrophages described in this paper was not mediated by LRP. Firstly, DiI-β-VLDL uptake in macrophages was sterol downregulated (see Fig. 2 *D*), whereas LRP biosynthesis in human fibroblasts was not sterol regulated. Secondly, DiI-β-VLDL uptake in macrophages was evident even though LDL receptor expression was maximal, whereas LRP-mediated β-VLDL uptake in human fibroblasts was only detectable in LDL receptor-negative cells. Lastly, apo E enrichment of β-VLDL was needed for LRP-mediated uptake in human fibroblasts, whereas DiI-β-VLDL did not require apo E enrichment for uptake by macrophages.

In fact, there is substantial evidence that LDL and β-VLDL do bind to the same receptor on macrophages (9, 21), and we have also observed that the two lipoproteins compete for

binding. Thus, other mechanisms are needed to explain the observed differences in endocytic patterns. Since LDL contains one ligand (apo B) per particle, whereas β-VLDL contains multiple (i.e., 10–15) ligands (apo E) per particle, receptor cross-linking (26) may be a signal for the differential sorting of β-VLDL. Examples of this idea include the routing of several recycling receptors, including transferrin (17) and LDL receptors (2), which can be altered by occupancy with multivalent ligands. Alternatively, receptor affinity itself may play a role in determining the pattern of endocytosis. For example, β-VLDL could remain receptor-associated for a longer time inside the cell (perhaps secondary to receptor–ligand dissociation of β-VLDL occurring at a lower pH [7]), allowing it to enter different endosomal compartments than LDL. Consistent with this idea was our finding that low affinity E2-β-VLDL gave a pattern of endocytosis similar to that of LDL (Fig. 7). However, since the E2-β-VLDL was not fully characterized (due to lack of sufficient material), it is also possible that the similarity of the endocytic patterns of LDL and E2-β-VLDL may be related to some other possible common feature of these two lipoproteins, such as particle size. Lastly, perhaps an intracellular binding protein is responsible for sequestering one of the ligands into a distinct pathway; in this regard, Beisiegel et al. (3) have recently described three intracellular proteins in liver (one of which has no known function yet) which bind apo E with high affinity.

The relevance of our biochemical and morphological data to the different potencies of the lipoproteins as ACAT stimulators is yet to be determined. β-VLDL stimulates ACAT much more than LDL when equal amounts of lipoprotein-cholesterol are added to the cells (Fig. 1). The finding that β-VLDL demonstrated less release of cholesterol from its CE core than LDL (Fig. 8) serves to highlight the fact that, per available cholesterol, β-VLDL is a much more potent ACAT stimulator than LDL. In fact, using ^{3}H-CE-labeled lipoproteins, we have determined that after 2 h of incubation, LDL delivers 2.4-fold more free cholesterol from its CE stores than β-VLDL, and yet β-VLDL stimulates ACAT 7-fold greater than LDL in this same time period (Xu, X.-X., and I. Tabas, manuscript in preparation). In addition, this finding raises the possibility that the free cholesterol component of β-VLDL (which accounts for ~10% of the particle's cholesterol content) may play a role in stimulating and/or providing substrate for ACAT.

Taken together, the morphological and biochemical data may suggest an alternative pathway of lipoprotein-mediated stimulation of ACAT in mouse peritoneal macrophages which differs significantly from previously documented pathways in other cells (e.g., human fibroblasts) (13). In human fibroblasts, for example, LDL protein and CE are rapidly delivered to and degraded in lysosomes, and the resultant liberation of free cholesterol is thought to stimulate ACAT (13). In mouse peritoneal macrophages, LDL is similarly rapidly degraded in lysosomes, but, for reasons unknown, the LDL-derived cholesterol does not stimulate ACAT. In contrast, β-VLDL is delivered to a set of widely distributed vesicles and is degraded much more slowly. However, this lipoprotein does markedly stimulate ACAT. One hypothesis to explain this scheme is that the distinct β-VLDL-containing vesicles possess some property (lacking in the LDL-containing vesicles) which render them ideally suited for the transfer of lipoprotein-derived cholesterol to ACAT. Perhaps this is nothing more than a proximity factor: if ACAT, which is known to be a microsomal enzyme (32), is located nearer to the widely distributed β-VLDL-containing vesicles than to the central LDL-containing vesicles, then diffusion of cholesterol from the β-VLDL vesicles to ACAT would be greatly facilitated. Alternatively, it is possible that the β-VLDL vesicles contain a protein or lipid that maximizes transfer of cholesterol to ACAT (or LDL-containing vesicles possess some property which targets their cholesterol to a cellular location [i.e., the plasma membrane] away from ACAT). Actual proof of this idea must await further characterization of the β-VLDL- and LDL-containing vesicles as well as other experiments that further correlate intracellular localization of lipoproteins with ACAT stimulation. However, regardless of any potential relevance of our data to ACAT stimulation and foam cell formation, the finding that LDL and β-VLDL have distinct endocytic patterns in mouse peritoneal macrophages should prove valuable for our further understanding of the mechanisms of endocytic sorting.

We thank Dr. Conrad Blum for referring to us the patient with familial dysbetalipoproteinemia and for performing the isoelectric focusing experiments on this patient's apo E. We are grateful to Laura Morse and Kristy Brown for providing technical assistance and to Dr. Carol Mason and Rich Blazesky for assistance in the electron microscopy.

This work was supported by National Institutes of Health grants HL-39703 and HL-21006 (I. Tabas) and DK-27083 (F. R. Maxfield). I. Tabas is an Established Investigator of the American Heart Association and Boehringer-Ingelheim, Inc.

Received for publication 1 September 1989 and in revised form 31 May 1990.

References

1. Ajioka, R. S., and J. Kaplan. 1987. Characterization of endocytic compartments using the horseradish peroxidase–diaminobenzidine density shift technique. *J. Cell Biol.* 104:77–85.
2. Andersen, R. G. W., M. S. Brown, U. Beisiegel, and J. L. Goldstein. 1982. Surface distribution and recycling of the LDL receptor as visualized by anti-receptor antibodies. *J. Cell Biol.* 93:523–551.
3. Beisiegel, U., W. Weber, J. R. Havinga, G. Ihrke, D. Y. Hui, M. E. Wernette-Hammond, C. W. Turck, T. L. Innerarity, and R. W. Mahley. 1988. Apolipoprotein E-binding proteins isolated from dog and human liver. *Arteriosclerosis.* 8:288–297.
4. Brown, M. S., and J. L. Goldstein. 1983. Lipoprotein metabolism in the macrophage: implications for cholesterol deposition in atherosclerosis. *Annu. Rev. Biochem.* 52:223–261.
5. Brown, M. S., S. E. Dana, and J. L. Goldstein. 1975. Receptor-dependent hydrolysis of cholesteryl esters contained in plasma LDL. *Proc. Natl. Acad. Sci. USA.* 72:2925–2929.
6. Carpentier, J.-L., P. Gorden, R. G. W. Anderson, J. L. Goldstein, M. S. Brown, S. Cohen, and L. Orci. 1982. Colocalization of ^{125}I-epidermal growth factor and ferritin-LDL in coated pits: a quantitative electron microscopic study in normal and mutant human fibroblasts. *J. Cell Biol.* 95:73–77.
7. Davis, C. G., J. L. Goldstein, T. C. Sudhoff, R. G. W. Anderson, D. W. Russel, and M. S. Brown. 1987. Acid-dependent ligand dissociation and recycling of LDL receptor mediated by growth factor homology region. *Nature (Lond.).* 326:760–765.
8. Deleted in proof.
9. Ellsworth, J. L, F. B. Kraemer, and A. D. Cooper. 1987. Transport of β-VLDL and chylomicron remnants by macrophages is mediated by the LDL receptor pathway. *J. Biol. Chem.* 262:2316–2325.
10. Faggioto, A., R. Ross, and L. Harker. 1984. Studies of hypercholesterolemia in the nonhuman primate. I. Changes that lead to fatty streak formation. *Arteriosclerosis.* 4:323–340.
11. Gerrity, R. G. 1981. The role of the monocyte in atherogenesis. I. Transition of blood-borne monocytes into foam cells in fatty lesions. *Am. J. Pathol.* 103:181–190.
12. Godement, P., J. Salaun, and C. A. Mason. 1990. Retinal axon pathfinding in the optic chiasm: divergence of crossed and uncrossed fibers. *Neuron.* In press.
13. Goldstein, J. L., and M. S. Brown. 1977. The low-density lipoprotein pathway and its relation to atherosclerosis. *Annu. Rev. Biochem.* 46:897–930.

14. Goldstein, J. L., Y. K. Ho, M. S. Brown, T. L. Innerarity, and R. W. Mahley. 1980. Cholesteryl ester accumulation in macrophages resulting from receptor-mediated uptake and degradation of hypercholesterolemic canine β-VLDL. *J. Biol. Chem.* 255:1839–1848.
15. Goldstein, J. L., S. K. Basu, and M. S. Brown. 1983. Receptor-mediated endocytosis of LDL in cultured cells. *Methods Enzymol.* 98:241–260.
16. Goldstein, J. L., M. S. Brown, R. G. W. Anderson, D. W. Russel, and W. J. Schneider. 1985. Receptor-mediated endocytosis: concepts emerging from the LDL receptor system. *Annu. Rev. Cell Biol.* 1:21–39.
17. Hopkins, C. R., and I. S. Trowbridge. 1983. Internalization and processing of transferrin and the transferrin receptor in human carcinoma A431 cells. *J. Cell Biol.* 97:508–521.
18. Hui, D. Y., T. L. Innerarity, and R. W. Mahley. 1984. Defective hepatic lipoprotein receptor binding of β-VLDL from type III hyperlipoproteinemic patients. Importance of apoprotein E. *J. Biol. Chem.* 259:860–869.
19. Innerarity, T. L., K. S. Arnold, K. H. Weisgraber, and R. W. Mahley. 1986. Apolipoprotein E is the determinant that mediates the receptor uptake of β-VLDL by mouse macrophages. *Arteriosclerosis.* 6:114–122.
20. Jaeckle, S., S. E. Brady, and R. J. Havel. 1989. Membrane binding sites for plasma lipoproteins on endosomes from rat liver. *Proc. Natl. Acad. Sci. USA.* 86:1880–1884.
21. Koo, C., M. E. Wernette-Hammond, and T. L. Innerarity. 1986. Uptake of canine β-VLDL by mouse peritoneal macrophages is mediated by a low density lipoprotein receptor. *J. Biol. Chem.* 261:11194–11201.
22. Kowal, R. C., J. Herz, J. L. Goldstein, V. Esser, and M. S. Brown. 1989. LDL receptor-related protein mediates uptake of cholesteryl esters derived from apoprotein E-enriched lipoproteins. *Proc. Natl. Acad. Sci. USA.* 86:5810–5814.
23. Lowry, O. H., N. J. Rosenbrough, A. L. Farr, and R. J. Randall. 1951. Protein measurement with the Folin reagent. *J. Biol. Chem.* 193:265–275.
24. Mahley, R. W., T. L. Innerarity, M. S. Brown, Y. K. Ho, and J. L. Goldstein. 1980. Cholesteryl ester synthesis in macrophages: stimulation by β-VLDL from cholesterol-fed animals of several species. *J. Lipid Res.* 21:970–980.
25. Maxfield, F. R., J. Schlessinger, Y. Schechter, I. Pastan, and M. C. Willingham. 1978. Collection of insulin, EGF and α_2-macroglobulin in the same patches on the surface of cultured fibroblasts and common internalization. *Cell.* 14:805–810.
26. Pitas, R. E., T. L. Innerarity, K. S. Arnold, and R. W. Mahley. 1979. Rate and equilibrium constants for binding of apo-E HDL and LDL to human fibroblasts: evidence for multiple receptor binding of apo-E HDL. *Proc. Natl. Acad. Sci. USA.* 76:2311–2315.
27. Pitas, R. E., T. L. Innerarity, J. N. Weinstein, and R. W. Mahley. 1981. Acetoacetylated lipoproteins used to distinguish fibroblasts from macrophages in vitro by fluorescence microscopy. *Arteriosclerosis.* 1:177–185.
28. Salzman, N. H., and F. R. Maxfield. 1988. Intracellular fusion of sequentially formed endocytic compartments. *J. Cell Biol.* 106:1083–1091.
29. Sandell, J. H., and R. Masland. 1988. Photoconversion of some fluorescent markers to a diaminobenzidine product. *J. Histochem. Cytochem.* 36: 555–559.
30. Schaffner, T., K. Taylor, E. J. Bantucci, K. Fischer-Dzoga, J. H. Beeson, S. Glagov, and R. Wissler. 1980. Arterial foam cells with distinctive immunomorphic and histochemical features of macrophages. *Am. J. Pathol.* 100:57–80.
31. Steinman, R. M., S. E. Brodie, and Z. A. Cohn. 1976. Membrane flow during pinocytosis. *J. Cell Biol.* 68:665–687.
32. Suckling, K. E., and E. F. Stange. 1985. Role of ACAT in cellular cholesterol metabolism. *J. Lipid Res.* 26:647–671.
33. Tabas, I., D. A. Weiland, and A. R. Tall. 1985. Unmodified LDL causes cholesteryl ester accumulation in J774 macrophages. *Proc. Natl. Acad. Sci. USA.* 82:416–422.
34. Tabas, I., D. A. Weiland, and A. R. Tall. 1986. Inhibition of ACAT in J774 macrophages enhances down-regulation of the LDL receptor and HMG-CoA reductase and prevents LDL-induced cholesterol accumulation. *J. Biol. Chem.* 261:3147–3155.
35. Tabas, I., G. C. Boykow, and A. R. Tall. 1987. Foam cell-forming J774 macrophages have markedly elevated ACAT activity compared with mouse peritoneal macrophages in the presence of LDL. *J. Clin. Invest.* 79:418–426.
36. Tabas, I., W. J. Rosoff, and G. Boykow. 1987. ACAT in macrophages utilizes a cellular pool of cholesterol oxidase-accessible cholesterol as substrate. *J. Biol. Chem.* 263:1266–1272.
37. Via, D. P., M. C. Willingham, I. Pastan, A. M. Gotto, Jr., and L. C. Smith. 1982. Co-clustering and internalization of LDL and α_2-macroglobulin in human skin fibroblasts. *Exp. Cell Res.* 141:15–22.
38. Ward, D. M., R. Ajioka, and J. Kaplan. 1989. Cohort movement of different ligands and receptors in the intracellular endocytic pathway of alveolar macrophages. *J. Biol. Chem.* 264:8164–8170.
39. Weisgraber, K., S. C. Rall, Jr., and R. W. Mahley. 1981. Human E apoprotein heterogeneity: cysteine-arginine interchanges in the amino acid sequence of the apo E isoforms. *J. Biol. Chem.* 256:9077–9083.